Available online at www.sciencedirect.com
ScienceDirect
Journal of the European Ceramic Society 29 (2009) 2651–2657
www.elsevier.com/locate/jeurceramsoc

Capillary infiltration studies of liquids into 3D-stitched C–C preforms Part B: Kinetics of silicon infiltration

Suresh Kumar [a,*], Anil Kumar [a], Rohini Devi [a], Anupam Shukla [b], A.K. Gupta [b]

[a] *Advanced Systems Laboratory (DRDO), Hyderabad 500058, India*
[b] *Department of Chemical Engineering, IIT Delhi, New Delhi 110016, India*

Received 11 October 2008; received in revised form 10 March 2009; accepted 12 March 2009
Available online 16 April 2009

Abstract

In Part A of this study, the details of 3D-stitched carbon–carbon (C–C) preform development and characterization of the internal pore structure have been described. A model based on pore radii of two sizes has been proposed for capillary infiltration of solvents in the C–C preforms. In the Part B, kinetics of silicon infiltration has been studied. Ten C–C preform bars of size 150 mm × 17 mm × 50 mm were siliconized at 1650 °C for different durations ranging from 6 to 180 s. Infiltration heights were measured by X-ray images of the siliconized bars. Formation of silicon carbide was incorporated in the model developed in Part A. Infiltration heights were estimated. These were in close agreement with the experimentally observed values.

Keywords: B. Composites; Silicon infiltration

1. Introduction

3D-carbon–silicon carbide (3D-C–SiC) composites exhibit better thermal and mechanical properties under severe erosion and complex mechanical loading. 3D-stitched C–SiC composites are easy to fabricate by liquid silicon infiltration (LSI) method and can be used for applications like jet-vanes, leading edges of hypersonic vehicles, etc. The pore structure of the composites depends upon the formation of silicon carbide due to infiltration of silicon. Understanding the kinetics of silicon infiltration in the preforms is the key to fabricate these composites. Experimental kinetic data available in literature for silicon infiltration are limited and are not applicable for the present system. Messner and Chiang[1] formulated an analytical model, based on Darcy's law[2]. The model considered varying permeability; it was used to predict the infiltration behavior of silicon through graphite preforms. In another study, an attempt was made to measure the silicon infiltration front velocity as a function of temperature[3]. Thin carbon tapes, fabricated by two different techniques were exposed to a silicon melt. Some studies on kinetics of silicon infiltration into porous carbon and 2D C–C preforms have also been reported in the literature[4–8].

In most cases mathematical analysis was carried out considering single mean effective pore radius. However, 3D-stitched C–C preforms have a wide distribution of pore sizes; this is because of the third direction reinforcement and non-uniform shrinkage of the carbon matrix during carbonization. The present work was undertaken to understand the capillary infiltration of liquids in such preforms.

In Part A of the present study, a model based on pore radii of two sizes has been proposed for capillary infiltration. In this part, kinetic studies for silicon infiltration are being presented.

The objectives are:

1. to carry out silicon infiltration into 3D-stitched C–C preform bars of 150 mm height for different durations;
2. to carry out microstructure analysis of the infiltrated specimens to understand the reaction mechanism between carbon and silicon;
3. to employ the model developed for solvent infiltration (in Part A of this study) for silicon infiltration kinetics.

* Corresponding author. Tel.: +91 40 24306498; fax: +91 40 24306498.
E-mail address: sureshtanwar@rediffmail.com (S. Kumar).

0955-2219/$ – see front matter © 2009 Elsevier Ltd. All rights reserved.
doi:10.1016/j.jeurceramsoc.2009.03.006

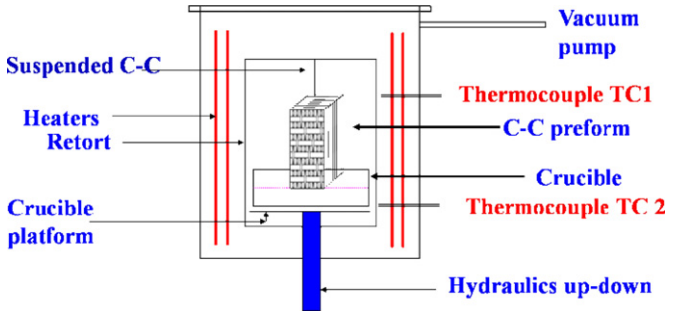

Fig. 1. Schematic of siliconization experimental set-up.

2. Experimental

Experimental details pertaining to fabrication and characterization of 3D-stitched C–C preform are already presented in the Part A. In this part, details pertaining to kinetics of silicon infiltration are given.

2.1. Silicon infiltration

Ten C–C preform bars each of length =150 mm, width = 17 mm, and thickness = 50 mm were siliconized at 1650 °C under vacuum (absolute pressure = 1×10^{-3} mmHg) for different time intervals; heating rate was maintained to achieve the temperature rise in the range of 10–15 °C/min. Siliconization was carried out in a top loading type vacuum furnace. There is a platform in the furnace located near the bottom. It can be raised or lowered by hydraulic means.

Procedure. A high density graphite crucible containing adequate quantity of silicon lumps was kept on the platform. One C–C bar was suspended inside the furnace (Fig. 1). The furnace was closed and vacuum was applied. The temperature in the furnace was raised at a pre-decided rate. Melting point of silicon is 1420 °C. After the furnace temperature reaches 1650 °C, the platform was raised to establish a contact between the C–C preform bar and molten silicon in the crucible. Liquid silicon rises in the C–C preform bar by capillary action. After a pre-decided infiltration time, the platform was lowered so that the preform bar and liquid silicon are no longer in contact and the furnace was switched off and allowed to cool. The furnace was opened and the siliconized bar was removed from the furnace at room-temperature.

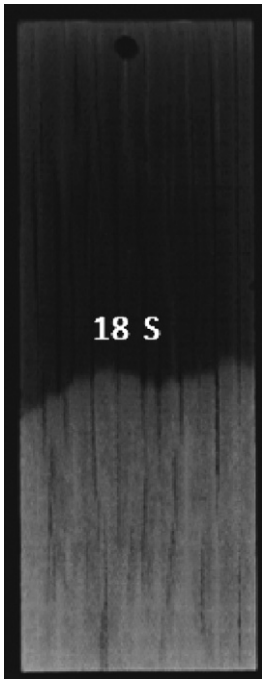

Fig. 2. Non uniform silicon infiltration front into 3D-stitched C–C preform bar.

2.2. Experimental observations

Silicon infiltrated in all the bars was determined by change in weight of the bars (Table 1). X-ray images of the bars were also taken (Figs. 2–4).

2.3. Measurements of silicon infiltration height

The images were taken at 160 kV with current density of 10 mA using Andrex Constant Potential X-ray set (model CP 490, 160 kV, focal spot 0.4 and 1.5). The distance between X-ray source and siliconized bars was maintained at 1 m to get contrast in the images. The silicon infiltrated portion is grey while the un-infiltrated part is dark black. The infiltrated part of the bars became hard. In some images it was observed that the infiltration front was not uniform across the thickness. It is perhaps due to the non-uniform local pore structure.

Infiltration height was calculated by taking five equally spaced points on the infiltration front. Height of each point was

Table 1
Silicon infiltration height and silicon uptake by C–C preform bars: kinetic study.

Bar no.	Initial weight of the bar (Wt_{start}), g	Infiltration time, s	Final weight of the bar (Wt_{final}), g	Silicon uptake, g	Infiltration height, m
Bar-1	195.0	6	205.5	10.5	0.032
Bar-2	200.0	18	226.0	26.0	0.066
Bar-3	201.5	24	228.5	27.0	0.070
Bar-4	198.0	30	226.0	28.0	0.072
Bar-5	204.5	36	234.0	29.5	0.074
Bar-6	206.5	48	244.5	38.0	0.088
Bar-7	200.5	90	247.5	47.0	0.118
Bar-8	201.0	108	252.0	51.0	0.121
Bar-9	199.0	138	255.0	56.0	0.126
Bar-10	199.5	180	267.0	67.5	0.148

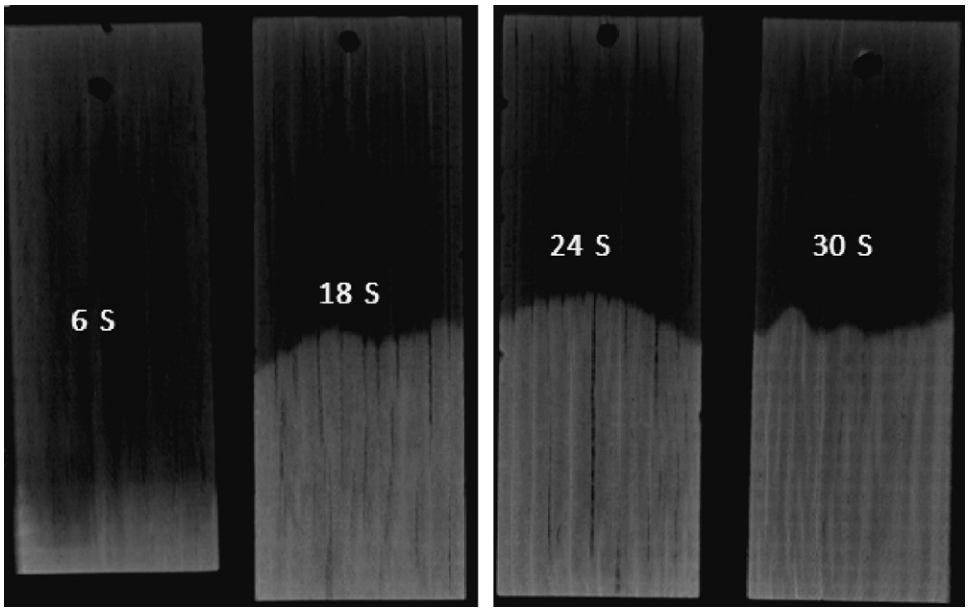

Fig. 3. X-ray images of C–SiC composite bars, siliconization time 6, 18, 24 and 30 s.

measured from the base. The arithmetic mean of the five values was taken as the effective infiltration height for that particular bar (Table 1).

It is interesting to note that silicon rose through a height of about 148 mm in only 180 s whereas it took almost 10,000 s for cyclohexanone (Part A). Higher rate of silicon infiltration is mainly due to its very high surface tension (0.72 N/m); for cyclohexanone it is 0.034 N/m.

3. Mathematical analysis

3.1. Reactive infiltration kinetics

Liquid silicon reacts with solid carbon matrix to form solid silicon carbide.

$$Si(l) + C(s) \rightarrow SiC(s)$$

It is envisaged that liquid silicon rises into the pores of the carbon matrix, where it reacts with the pore walls to form silicon carbide; the diameter of the pores thus reduces.

Microstructure analysis of C–SiC composite bars was carried out to understand the reaction mechanism. Parts of the siliconized bars (bar-4 and bar-10, respectively) were cut and polished. Their microstructure was seen under an optical microscope (Figs. 5 and 6).

1. Continuous and non-uniform thick SiC layer could be observed over the carbon phase.
2. Some SiC particles embedded in the silicon pool and located away from the carbon phase were also visible.

The following mechanisms of SiC formation have been proposed in the literature[4,9–11].

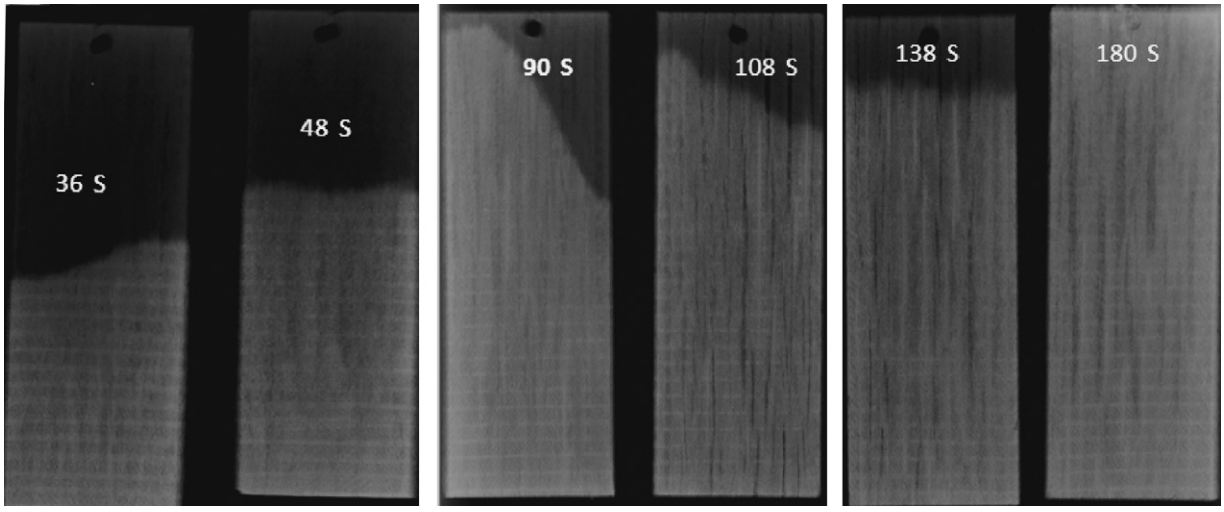

Fig. 4. X-ray images of C–SiC composite bars, siliconization time 36 and 48, 90, 108, 138 and 180 s.

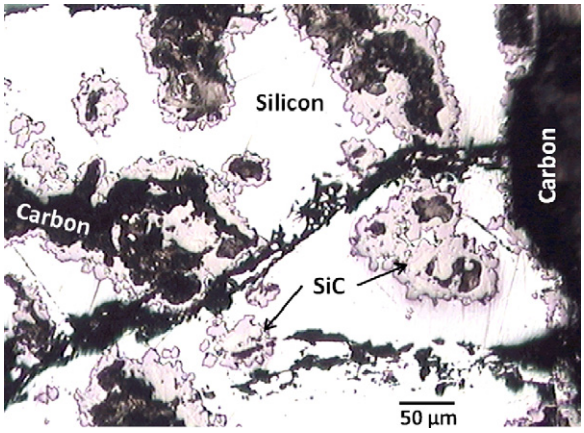

Fig. 5. Optical micrograph-1 of C–SiC bar (4) siliconized for (30 s).

(i) Heterogeneous nucleation and growth of SiC leads to the formation of a continuous polycrystalline SiC layer; its further growth is attributed to diffusion of the reactive species through SiC layer[4].
(ii) Carbon dissolves in liquid silicon instantaneously, leading to the formation of SiC clusters which are preferentially adsorbed on the liquid/solid interface[9]. After saturation of this adsorption layer by the SiC clusters, a two-dimensional continuous SiC film is formed.
(iii) A continuous layer of SiC precipitates in the silicon phase. It is proposed that diffusion of carbon through the SiC layer is the rate limiting step.
(iv) Solution precipitation mechanism has been proposed by Pampuch *et al.*[11]. Carbon dissolves in liquid silicon and silicon carbide is formed which subsequently precipitates. Both dissolution of carbon and formation of SiC are exothermic; the heat of the dissolution is −247 kJ/mol, and the heat of reaction is −115 kJ/mol. Thus, temperature at the reaction site is likely to be higher than the local surrounding temperature.

It was inferred from the literature that the initial formation of SiC layer is very fast it precipitates, and its subsequent growth is controlled by diffusion of silicon through it. It may also be noted that there is a volume misfit between carbon and the product SiC

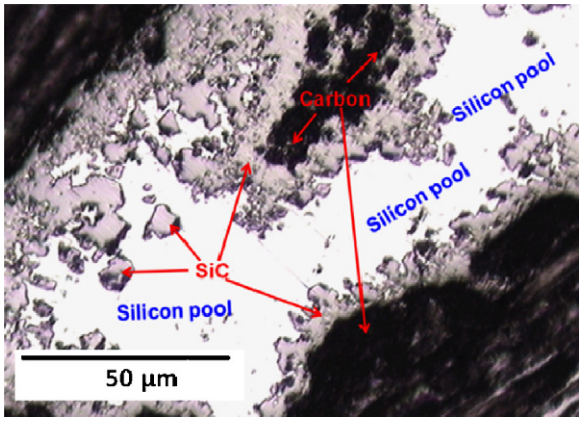

Fig. 6. Optical micrograph-2 of C–SiC bar (10) siliconized for (180 s).

[3]. Therefore, some of the SiC formed may break into small particles and move to liquid silicon pool. If so, molten silicon would be in contact with fresh carbon to react. Thus SiC formation may also be an interface-limited reaction between carbon and silicon.

3.2. Mathematical analysis

As mentioned earlier, liquid silicon rises into pores of the preform. Also, the pore size would decrease with time as solid SiC formed and gets deposited on the walls of the pores. The SiC layer inside the pores would be thickest at the mouth of the pore at the bottom and would be negligible at the top of the infiltrated height. It may be noted that capillary infiltration depends upon pore radius.

(a) *Thickness of SiC layer on flat horizontal carbon surface*: The rate of reaction between carbon and silicon melt is extremely fast as compared to the rate of diffusion of liquid silicon in the solid SiC, the diffusion of silicon would be the rate controlling step. This concept has been applied to analyze silicon infiltration kinetic data.

If a flat carbon surface is in contact with molten silicon, it can be shown that, thickness of SiC layer would be given by

$$\delta = \sqrt{\left(\frac{2D}{\rho} C_{Si,l}\right)}\sqrt{t} \tag{1}$$

where δ = thickness of silicon carbide layer, m, ρ = density of silicon carbide, kg/m^3, D = diffusion coefficient of Si through SiC layer, m^2/s, $C_{Si,l}$ = density of silicon in the liquid phase, kg/m^3, t = reaction time, s

The derivation is given in the Appendix A.

Physical properties of carbon–silicon system are given in Table 2.[6] Substituting for the values, we get

$$\delta = 2.843 \times 10^{-7}\sqrt{t} \tag{1a}$$

The thickness of SiC layer would grow in the two opposite directions away from the SiC–silicon interface: (i) in the pool of molten silicon, (ii) into the thickness of carbon matrix (Fig. A.1). It is also shown in Appendix A that, the thickness created in the liquid silicon pool is 0.561δ.

3.2.1. Diffusion-limited capillary rise

As mentioned earlier, radius of the pore decreases due to the formation of SiC inside the capillary. The thickness of SiC layer δ grows outward in the carbon matrix and on the other hand, it grows towards the centre of the pore in the liquid silicon pool. It can be shown that the capillary radius for carbon–silicon reactive system at any time would be given by

$$r(t) = r_0 - 0.561\delta \tag{2}$$

where, r_0 is the radius at $t = 0$.

Thus Eq. (2) can be rewritten as

$$r(t) = r_0 - 0.561 \times 2.843 \times 10^{-7}\sqrt{t} \tag{3}$$

Table 2
Physical properties of silicon used in this study.

Properties	Units	Literature	Values used in the present study
Density	kg/m^3	2330–2340 (20°C) 2530–2550 (1420°C)	2500
Viscosity	kg/m s	5.10×10^{-4} to 7.65×10^{-4} (1440 °C) 4.59×10^{-4} to 6.38×10^{-4} (1560 °C)	7.65×10^{-4}
Contact angle	°	0–22 (silicon versus carbon in vacuum)	22
Surface tension	N/m	0.72–0.75 (1550 °C)	0.72

or,

$$r(t) = r_0 - 1.594 \times 10^{-7}\sqrt{t} \tag{3a}$$

In general, $r(t)$ may be represented as

$$r(t) = r_0 - M\sqrt{t} \tag{4}$$

Eq. (4) has also been reported in the literature[8] with the value of M to lie in the range of 0.4×10^{-7} to 2×10^{-7} m s$^{-1/2}$. Larger value of M implies quicker reduction in pore radius.

(b) *Capillary infiltration height*: In Part A, the model developed for solvent infiltration into the C–C preform was based on two pore radii.

$$\frac{8\mu}{r_2^2}\frac{hdh}{dt} - \frac{2\sigma\cos\theta}{r_1} + \rho g h = 0 \quad \text{(equation 15 of Part A)} \tag{5}$$

It may be recalled that for solvent infiltration, $r_{1,0}$ and $r_{2,0}$ were found to be 34.2 and 4.3 μm, respectively.For reactive infiltration of silicon, as discussed above

$$r_1(t) = r_{1,0} - M\sqrt{t} \tag{6}$$

$$r_2(t) = r_{2,0} - M\sqrt{t} \tag{7}$$

Thus $r_1(t)$ and $r_2(t)$ can be determined. The effect of $M\sqrt{t}$ becomes pronounced with reduction in pore size and with time. This also indicates smaller pores would be susceptible to choking soon after silicon infiltration has started, and with passage of time, less and less pores would be available for silicon infiltration.

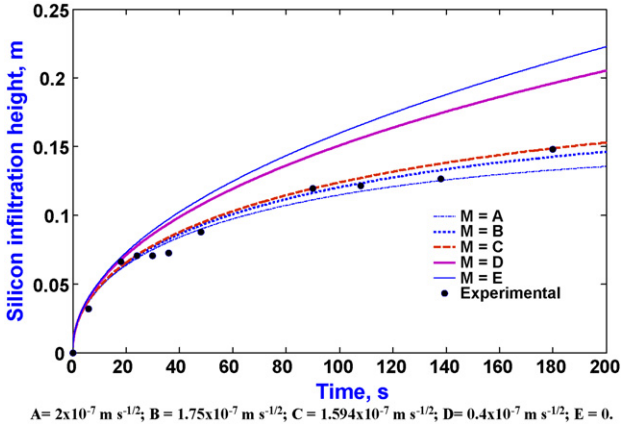

Fig. 7. Comparison of experimental and estimated silicon infiltration heights by modified Washburn equation (contact angle 22°).

Eq. (5) was solved numerically (by Runge Kutta method) to estimate silicon infiltration height as a function of time. The angle of contact θ was assumed to be 22°[6,8,12]. Calculations were performed for different values of M.

(a) $M = 2 \times 10^{-7}$ m s$^{-1/2}$;
(b) $M = 1.75 \times 10^{-7}$ m s$^{-1/2}$;
(c) $M = 1.594 \times 10^{-7}$ m s$^{-1/2}$;
(d) $M = 0.4 \times 10^{-7}$ m s$^{-1/2}$;
(e) $M = 0$.

The results are shown in Fig. 7.

It can be seen that $M = 0$ overestimates the infiltration height while $M = 2.0 \times 10^{-7}$ m s$^{-1/2}$ underestimates the same; $M = 1.594 \times 10^{-7}$ m s$^{-1/2}$ estimates the heights reasonably close to the experimental data; however the best correlation is obtained for $M = 1.75 \times 10^{-7}$ m/s$^{1/2}$. For $M = 1.75 \times 10^{-7}$ m/s$^{1/2}$, the values of $r_1(t)$ and $r_2(t)$ at 180 s are 31.85 and 1.95 μm, respectively. It means that capillary pressure ($2\sigma\cos\theta/r_1$) increases marginally with time, and at the same time, viscous drag ($(8\mu/r_2^2)(hdh/dt)$) increases significantly.

As mentioned earlier, the SiC layer inside the pores at any instant would not be uniformly thick: the maximum thickness would be at the mouth of pores at the bottom, and the thickness would be negligible at the top of the infiltrated height. However, Eq. (5) assumes uniform thickness throughout the infiltrated height in the pores, and is equal to that at the pore mouth.

3.2.2. Variable angle of contact

As mentioned earlier, the C–C preform bar was just touching the molten silicon. The silicon rises in the pores and reacts with carbon matrix. The carbon–silicon reaction is very fast; therefore, at the bottom of the bar, SiC layer forms almost instantaneously. From Eq. (5), it is evident that the angle of contact between SiC layer and silicon plays an important role for silicon infiltration. The angle of contact varies from 0 to 22° under vacuum and also varies with reaction time[8,12,13].

$$\theta(t) = \theta_\infty + \theta_\infty(\exp(B - At)) \tag{8}$$

where $\theta(t)$ is the angle of contact between molten silicon and pore wall at any time 't'; θ_∞ is the angle of contact at equilibrium (4.2°); B is the material constant (1.68); A is the material constant (0.00543 s^{-1}).

The values of θ at $t = 0$ and $t = 180$ s are 26.73° and 6.22°, respectively; the corresponding values of $\cos\theta$ are 0.893 and

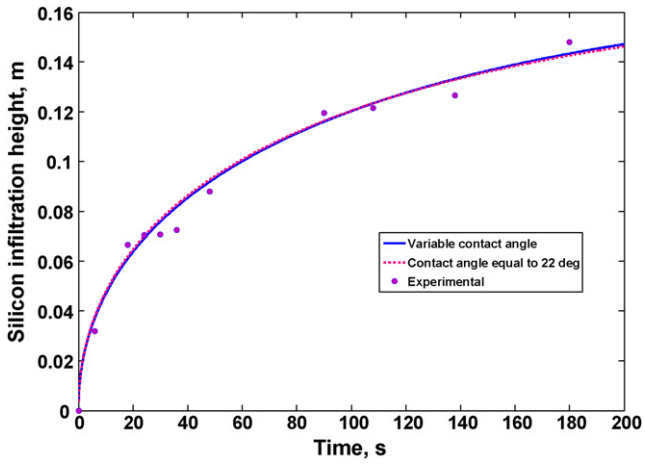

Fig. 8. Comparison of estimated heights obtained from variable angle of contact and contact angle = 22° for $M = 1.75 \times 10^{-7}$ m s$^{-1/2}$.

0.994, respectively. Thus computations were performed taking into account the change in contact angle θ with time t (Fig. 8). It is evident that with $\theta = 22°$ and with $\theta(t) = \theta_\infty + \theta_\infty(\exp(B - At))$ the estimated infiltration heights are almost the same.

4. Concluding remarks

Combining the findings of both the parts, A and B of this study, following conclusions may be drawn

(i) The capillary infiltration of a solvent in the C–C preform may be correlated by modified Washburn equation. It is based on pores of two radii $r_{1,0}$ and $r_{2,0}$: $r_{1,0}=2\sigma\cos\theta/\rho g h_{t\to\infty}$, and $r_{2,0}$ may be obtained by analyzing the experimental data with the help of modified Washburn equation.

(ii) The infiltration height of molten silicon in the C–C preform may be estimated using the same equation and substituting $r_1(t) = r_{1,0} - 1.75 \times 10^{-7}\sqrt{t}$ m and $r_2(t) = r_{2,0} - 1.75 \times 10^{-7}\sqrt{t}$ m.

Appendix A. Determination of *M* for flat geometry

(a) *Physical picture envisaged*

1. A pool of molten silicon is brought into contact with a horizontal flat slab of carbon. Reaction takes place between silicon and carbon to form a layer of silicon carbide. Thickness of silicon carbide layers grows with time. A schematic of SiC layer formation is shown in Fig. A.1.

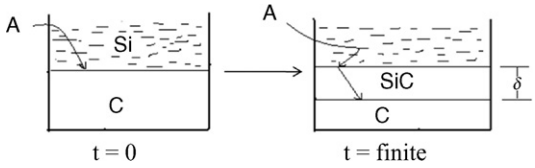

Fig. A.1. Schematic of SiC layer formation at flat graphite plate.

$$\mathrm{Si(l)} + \mathrm{C(s)} \rightarrow \mathrm{SiC(s)}$$

2. After the formation of initial layer of silicon carbide, liquid silicon must diffuse through silicon carbide layer to reach carbon surface to form fresh silicon carbide, immediately. If we assume SiC formation reaction as instantaneous, molten silicon cannot exist at the interface of the carbon and silicon carbide layer.

(b) *Mathematical analysis*: Assumption: quasi steady state

$$m = \delta\rho A \tag{1A}$$

where m = mass of SiC layer formed during time t, kg, δ = thickness of silicon carbide layer, m, ρ = density of silicon carbide, kg/m^3, A = interfacial area between molten silicon and carbon, m^2

$$\frac{dm}{dt} = \rho A\frac{d\delta}{dt} \tag{2A}$$

dm/dt = mass of silicon carbide formed per unit time, kg/s

Expressing rate of formation of SiC in terms of diffusion flux

$$\frac{dm}{dt} = A\frac{D}{\delta}(C_{Si,l} - C_{Si,i}) \tag{3A}$$

D = diffusion coefficient of Si through SiC layer, m^2/s, $C_{Si,l}$ = concentration of silicon in the liquid phase, kg/m^3, $C_{Si,i}$ = concentration of silicon at silicon carbide–carbon interface (=0), kg/m^3

Equation (3A) reduces to

$$\frac{dm}{dt} = A\frac{D}{\delta}C_{Si,l} \tag{4A}$$

From (2A) and (4A) above

$$\delta\frac{d\delta}{dt} = \frac{D}{\rho}C_{Si,l} \tag{5A}$$

Integrating (5A)

$$\delta^2 = \frac{2D}{\rho}C_{Si,l}t + \text{constant} \tag{6A}$$

At $t = 0$, $\delta = 0$, i.e., constant = 0; Eq. (6A) would reduce to

$$\therefore \delta^2 = \frac{2D}{\rho}C_{Si,l}t \tag{7A}$$

or

$$\delta = \sqrt{\frac{2D}{\rho}C_{Si,l}\sqrt{t}}$$

$$D = D^\circ\, \mathrm{e}^{-E/RT}\mathbf{4}$$

where E is the activation energy = 132 kJ/mol; $D^{\circ} = 2.0 \times 10^{-6}\,\mathrm{cm^2/s}$.

At siliconization temperature of 1650 °C, D comes out to be $5.194 \times 10^{-10}\,\mathrm{cm^2/s}$.

Substituting for $C_{Si,l}$, D and ρ in equation (7A)

$C_{Si,l} = 2500\,\mathrm{kg/m^3}$, $\rho = 3217\,\mathrm{kg/m^3}$, $D = 5.194 \times 10^{-14}\,\mathrm{m^2/s}$, $\delta = 2.841 \times 10^{-7}\sqrt{t}$

(c) *Determination of M (thickness of new SiC layer created)*: In the formation of SiC, one mole of solid carbon produces one mole of SiC

	C	+	Si	→	SiC
Molecular weight	12		28		40
Density, g cm^{-3}	2.2		2.5		3.217
Volume, cm^3	5.45		11.2		12.43

$$\text{New volume created} = 12.43 - 5.43 = 6.98\,\mathrm{cm^3}$$

$$\frac{\text{New volume formed}}{\text{Total volume of SiC produced}} = \frac{6.98}{12.43} = 0.561$$

Thus a flat vertical wall of carbon in contact with a pool of liquid silicon will produce new thickness as shown by above calculations.

$$\delta = M\sqrt{t} \tag{A.8}$$

$$\begin{aligned} M &= \frac{\text{new solid volume created}}{\text{volume of SiC thickness layer}} \times \sqrt{\frac{2D}{\rho}} C_{Si,l} \\ &= 0.561 \times 2.843 \times 10^{-7} \\ &= 1.594 \times 10^{-7}\,\mathrm{m\,s^{-1/2}} \end{aligned} \tag{A.9}$$

References

1. Messner, R. P. and Chiang, Y. M., Liquid-phase reaction-bonding of silicon carbide using alloyed silicon-molybdenum melts. *J. Am. Ceram. Soc.*, 1990, **73**, 1193–1200.
2. Darcy, H. P. G., *Les fontaines publiques de la ville de Dijon, Expositionet application des principles a suivre et des formules a employer dans les questions de distribution deau*. Victor Dalmont, Paris, 1856.
3. Einset, E. O., Capillary infiltration rates into porous media with applications to silicomp processing. *J. Am. Ceram. Soc.*, 1996, **79**, 333–338.
4. Fitzer, E. and Gadow, R., Fibre-reinforced silicon carbide. *Am. Ceram. Soc. Bull.*, 1986, **65**, 326–335.
5. Martin, G. P., Olson, D. L. and Edwards, G. R., Modeling of infiltration kinetics for liquid metal processing of composites. *Metall. Trans. B*, 1988, **19B**, 95–101.
6. Gern, F. H. and Kochendorfer, R., Liquid silicon infiltration description of infiltration dynamics and silicon carbide formation. *Comp. Part A*, 1997, **28A**, 355–364.
7. Sangsuwan, P., Tewari, S. N., Gatica, J. E., Singh, M. and Dickerson, R., Reactive infiltration of silicon melt through microporous amorphous carbon preform. *Metall. Mater. Trans. B*, 1999, **30b**, 933–944.
8. Asthana, R., Interface- and diffusion-limited capillary rise of reactive melts with a transient contact angle. *Metall. Mater. Trans. A*, 2002, **33A**, 2119–2128.
9. Li, J. G. and Hausner, H., Wetting and infiltration of graphite materials by molten silicon. *Scripta Metall. Mater.*, 1995, **32**, 377.
10. Zhou, H. and Singh, R. N., Kinetics model for the growth of silicon carbide by the reaction of liquid silicon with carbon. *J. Am. Ceram. Soc.*, 1995, **78**, 2456–2462.
11. Pampuch, R., Walasek, E. and Bialoskorski, J., Reaction mechanism in carbon–liquid silicon systems at elevated temperature. *Ceram Int.*, 1986, **12**, 99–106.
12. Asthana, R., Dynamic wetting effects during infiltration of metals. *Scripta Mater.*, 1998, **38**, 1203–1210.
13. Asthana, R., An analysis for spreading kinetics of liquid metals on solids. *Metall. Mater. Trans. A*, 1995, **26A**, 1307–1310.